Demonstration of Brillouin Distributed Discrimination of Strain and Temperature Using a Polarization-Maintaining Optical Fiber

Weiwen Zou, *Member, IEEE*, Zuyuan He, *Member, IEEE*, and Kazuo Hotate, *Fellow, IEEE*

***Abstract*—Distributed discrimination of strain and temperature is demonstrated by localizing both the stimulated Brillouin scattering (SBS) and the dynamic acoustic grating generated in the SBS process in a polarization-maintaining fiber with a correlation-domain continuous-wave technique. A 12-$\mu\varepsilon$ strain resolution and 0.3 °C temperature resolution together with a 10-cm spatial resolution are experimentally validated.**

***Index Terms*—Brillouin scattering, dynamic grating, fiber-optic sensors, polarization-maintaining fiber (PMF), strain, temperature.**

I. Introduction

FIBER-OPTIC distributed sensing systems based on Brillouin scattering have been regarded as powerful tools to monitor the distribution of strain and temperature in smart materials and structures [1], [2]. To determine the strain and the temperature simultaneously, we proposed recently a novel method by measuring both the Brillouin frequency shift (ν_B) and the birefringence (B) in a polarization-maintaining fiber (PMF) [3]. Because the two parameters are physically independent, this method ensures a complete discrimination of the strain and the temperature with much higher accuracy than those reported methods based on measuring multiple resonant frequencies of stimulated Brillouin scattering (SBS) in specially designed optical fibers [4]–[7]. The birefringence in the PMF was precisely determined by measuring the dynamic acoustic grating spectrum (DGS) generated in the SBS process [8] where the central frequency deviation (f_{yx}) is proportional to the birefringence [3], [8]. Most recently, we proposed further two individual methods to localize the dynamic acoustic grating to measure the distribution of the DGS along the fiber. One is based on the correlation-domain continuous-wave (CW) technique [9] and the other on the time-domain pulse-based technique [10].

In [3], the discrimination technique was demonstrated for the total strain and the total temperature over an entire 32-m-long PMF. In this letter, by integrating this discrimination technique with the scheme of distributed DGS measurement [9] and with the Brillouin optical correlation-domain analysis technique [2], we demonstrate for the first time the distributed discrimination of the strain and the temperature along a single-length optical fiber.

In the experiment, the local Brillouin gain spectrum (BGS) and DGS changes induced by applied-strain and/or temperature variation at a 12-cm-long PMF portion were clearly distinguished. Distributed discrimination of strain and temperature along an 8-m-long PMF was realized by measuring the local BGS and DGS successively with 10-cm spatial resolution.

II. Experiments

The experiment setup is similar to that explained in detail in [9]. Two ∼1550-nm distributed-feedback laser diodes (LDs) under sinusoidal frequency modulations were used as the light sources. LD1 was used for pump and probe waves to generate and localize the SBS and the dynamic acoustic grating at an arbitrary position within the PMF; LD2 for readout of the localized dynamic acoustic grating. The frequency of the probe was linearly swept by using a single sideband modulator to measure the localized BGS, while the frequency of LD2 was linearly swept to measure the localized DGS. The spatial resolutions (Δz_B and Δz_D) in BGS and DGS measurements are determined by [9]

$$\Delta z_B = d_m \frac{\Delta \nu_B}{\pi \Delta f_B} \tag{1}$$

$$\Delta z_D = d_m \frac{\Delta f_{yx}}{\pi \Delta f_D} \tag{2}$$

where $\Delta\nu_B =\sim 30$ MHz is the linewidth of BGS, $\Delta f_{yx} =\sim 300$ MHz the linewidth of DGS. Δf_B is the modulation depth of LD1 for localizing SBS in BGS measurement, Δf_D the modulation depth of both LDs for localizing the dynamic acoustic grating in DGS measurement. d_m is the measurement range determined by [9]

$$d_m = \frac{c}{2n_{\text{eff}} f_m} \tag{3}$$

where $n_{\text{eff}} = 1.446$ is the effective refractive index of the PMF, f_m the modulation frequency of the lasers, and c the light speed in vacuum.

Manuscript received December 06, 2009; accepted January 23, 2010. First published February 22, 2010; current version published March 17, 2010. This work was supported by the "Grant-in-Aid for Scientific Research (S)" and by the "Global Center of Excellence Program" from the Ministry of Education, Culture, Sports, Science and Technology (MEXT), Japan.

W. Zou was with the Department of Electrical Engineering and Information Systems, the University of Tokyo, Tokyo 113-8656, Japan, and is now with the Department of Electronic Engineering, Shanghai Jiao Tong University, Shanghai 200240, China (e-mail: zou@sagnac.t.u-tokyo.ac.jp).

Z. He and K. Hotate are with the Department of Electrical Engineering and Information Systems, the University of Tokyo, Tokyo 113-8656, Japan (e-mail: ka@sagnac.t.u-tokyo.ac.jp; hotate@sagnac.t.u-tokyo.ac.jp).

Color versions of one or more of the figures in this letter are available online at http://ieeexplore.ieee.org.

Digital Object Identifier 10.1109/LPT.2010.2041922

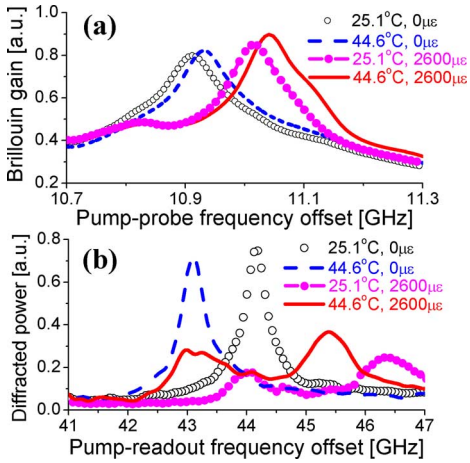

Fig. 1. (a) Measured examples of the local BGS and (b) the local DGS when the sensing position was localized at the 12-cm PMF portion, upon which a longitudinal strain ($\sim$2600 $\mu\varepsilon$) and/or a temperature increase ($\sim$19.5 °C) was applied.

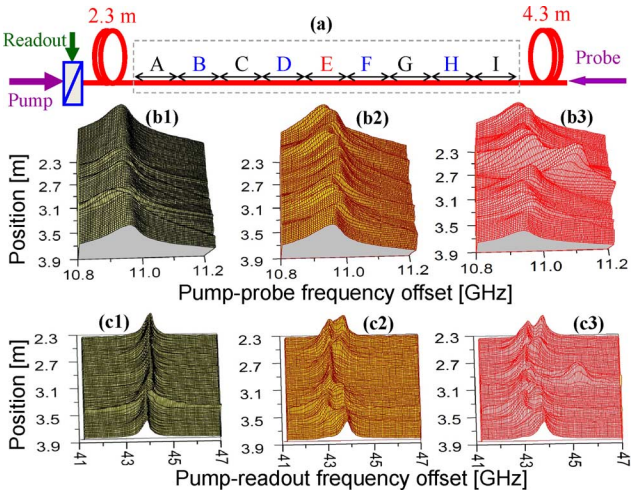

Fig. 2. (a) PMF sample comprising nine cascaded strained and heated fiber portions (dashed box) with 10–16 cm in length. (b1)–(b3) The 3-D distribution of the measured BGS, and (c1)–(c3) the 3-D distribution of the measured DGS. In (b1) and (c1), all fiber portions were laid freely at 25.1 °C. In (b2) and (c2), the portions B, D, E, F, and H were heated by $\Delta T = 19.5$ °C in loose state. In (b3) and (c3), the same portions were heated in loose state but the E portion was additionally strained by $\Delta\varepsilon =\sim 2600\ \mu\varepsilon$.

In the experiment, the LD modulation frequency was set to $f_m = 12.429$ MHz, which determines the nominal measurement range as $d_m = 8.35$ m according to (3). For local BGS measurement, the modulation depth of LD1 was set to $\Delta f_B =$ 1.5 GHz corresponding to a nominal spatial resolution $\Delta z_B =$ 5 cm according to (1). The pump–probe frequency offset was ramp-swept from 10.7 to 11.3 GHz at a rate of $\sim$10 Hz to collect the local BGS. The local Brillouin frequency shift ν_B was evaluated by Lorentzian-fitting or peak-searching on the collected BGS. For the local DGS measurement, the pump–probe frequency offset was fixed at the Brillouin frequency shift ν_B obtained above, while the modulation depths of the two LDs were both set to the most achievable value of the LDs as $\Delta f_D =$ 10 GHz corresponding to a nominal spatial resolution $\Delta z_D =$ 8 cm according to (2). The pump-readout frequency offset was linearly scanned from 41 to 47 GHz at a rate of $\sim$10 Hz to collect the local DGS. The local frequency deviation f_{yx} was evaluated by Gaussian fitting or peak-searching on the collected DGS. The measurement speed of the local BGS and the local DGS at one position is about 2 Hz. The pump, probe, and readout powers were about 26, 3, and 23 dBm, respectively.

At first, we selected a 12-cm fiber portion within a $\sim$8-m PMF as the sensing point by adjusting the LD modulation frequency f_m. Upon the 12-cm fiber portion, a tensile strain ($\Delta\varepsilon =\sim 2600\ \mu\varepsilon$) and/or a temperature increment ($\Delta T =\sim 19.5$ °C) were applied. The measured BGS and DGS at the 12-cm fiber portion are summarized in Fig. 1(a) and (b), respectively. Fig. 1(a) shows that the local Brillouin frequency shift ν_B is increased by either the strain or the temperature with respect to the reference at 25.1 °C and in loose state. On the other hand, as shown in Fig. 1(b), the strain increases but the temperature increment decreases the frequency deviation f_{yx}. When the strain and the temperature increment were simultaneously applied, the local Brillouin frequency shift ν_B is increased by both the strain and the temperature. However, the local frequency deviation f_{yx} is increased by the strain, and decreased by the temperature increment. These results match well with our previous report over an entire $\sim$32-m PMF [3].

To validate the feasibility of distributed discrimination of strain and temperature, we constructed a $\sim$8-m PMF sample consisting of nine (A–I) cascaded fiber portions of 10–16 cm in length, which is illustrated in Fig. 2(a). The A, C, G, and I portions were loosely laid at 25.1 °C for reference, while the B, D, F, and H portions were loosely inserted into a temperature-controlled water bath with 0.1 °C accuracy. The E portion was also inserted into the water bath and glued to a set of translation stages to load strain.

To perform distributed discrimination of strain and temperature along the cascaded strained and heated fiber portions, we repeated the above measurements of the local BGS and DGS (see Fig. 1) by resetting different LD modulation frequencies from 12430.484 to 12441.258 kHz with a step of 144 Hz, which corresponds to the fiber location from 2.35 to 3.85 m with a step of 2 cm. All the operations were automatically controlled by LabVIEW programs.

The three-dimensional (3-D) distribution of the measured BGS and DGS are summarized in Fig. 2(b1)–(b3) and (c1)–(c3), respectively. Even when all the cascaded fiber portions were loosely laid at 25.1 °C (around room temperature), the measured results show that both the BGS and the DGS are fluctuated along the fiber [Fig. 2(b1) and (c1)]. This is due to the bending-induced strain fluctuation along the PMF. When the B, D, E, F, and H portions were heated in loose state to 44.6 °C, the BGS at the heated portions [Fig. 2(b2)] shifts to the higher frequency, but the DGS [Fig. 2(c2)] moves to the lower frequency. When the E portion was further strained by $\Delta\varepsilon =\sim 2600\ \mu\varepsilon$, its BGS [Fig. 2(b3)] was shifted further to the higher frequency, but the DGS [Fig. 2(c3)] was reversed to shift to the higher frequency. The corresponding distribution of the change of the Brillouin frequency shift ($\Delta\nu_B$) and that of the frequency deviation (Δf_{yx}) were obtained by peak-searching the 3-D BGS and DGS. The results are summarized in Fig. 3(a) and (b), respectively.

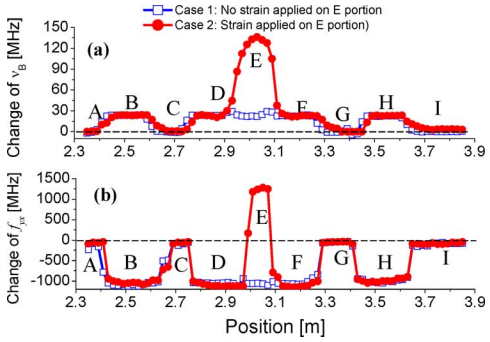

Fig. 3. (a) Distribution of the change of the Brillouin frequency shift ν_B and (b) the frequency deviation f_{yx}. Open squares: portions B, D, E, F, and H were heated in loose state by $\Delta T = 19.5$ °C. Solid circles: same portions were heated in loose state and the E portion was additionally strained by $\Delta\varepsilon = \sim 2600\ \mu\varepsilon$. The horizontal lines (dashed) correspond to the zero changes.

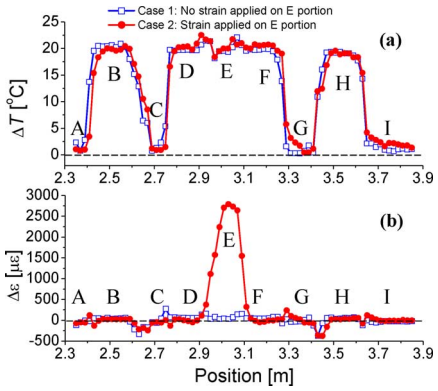

Fig. 4. Distributed discrimination of (a) strain and (b) temperature. Open squares: portions B, D, E, F, and H were heated in loose state by $\Delta T = 19.5$ °C. Solid circles: same portions were heated in loose state and the E portion was additionally strained by $\Delta\varepsilon = \sim 2600\ \mu\varepsilon$. The horizontal lines (dashed) correspond to the zero changes.

Referred to the strain ($C_\nu^\varepsilon = +0.03938$ MHz/$\mu\varepsilon$ and $C_f^\varepsilon = +0.8995$ MHz/$\mu\varepsilon$) and temperature ($C_\nu^T = +1.0580$ MHz/°C and $C_f^T = -55.8134$ MHz/°C) coefficients of $\Delta\nu_B$ and Δf_{yx} in the same kind of PMF [3], the local strain ($\Delta\varepsilon$) and the local temperature (ΔT) can be deducted by

$$\begin{pmatrix}\Delta\varepsilon\\ \Delta T\end{pmatrix} = \frac{1}{C_\nu^\varepsilon\cdot C_f^T - C_\nu^T\cdot C_f^\varepsilon}\begin{pmatrix}C_f^T & -C_\nu^T\\ -C_f^\varepsilon & C_\nu^\varepsilon\end{pmatrix}\begin{pmatrix}\Delta\nu_B\\ \Delta f_{yx}\end{pmatrix}. \quad (4)$$

Fig. 4 summarizes the deducted distribution of strain and temperature along the fiber, which clearly shows the feasibility of distributed discrimination of strain and temperature. No matter the strain is applied or not applied on the portion E, the temperature distribution along the PMF keeps the same [see Fig. 4(a)]. As shown in Fig. 4(b), the strain applied on E is clearly distinguished. It is noticeable that there is a little distinction between the preset values and the measured results of the strain and the temperature. This distinction is possibly due to the fact that the strain and temperature along the PMF sample was not applied precisely enough to the preset values.

The system accuracy was further testified by a repeatability test. The standard errors were measured to be ~0.5 MHz for the Brillouin frequency shift ν_B and ~10.8 MHz for the frequency deviation f_{yx}. According to (4), the accuracies of the distributed discrimination of strain and temperature were estimated as high as ~12 $\mu\varepsilon$ and ~0.3 °C, respectively.

III. Conclusion

We have demonstrated the correlation-domain distributed discriminative sensing of strain and temperature using a PMF. The distributions of the Brillouin frequency shift change ($\Delta\nu_B$) and the frequency deviation change (Δf_{yx}) along the PMF were experimentally measured by continuously accessing the sensing portions with a spatial resolution of ~10 cm. The simultaneously applied strain and temperature distributions were successfully discriminated by use of the measured $\Delta\nu_B$ and Δf_{yx}. According to repeatability test, the discriminative accuracies are estimated as high as 12 $\mu\varepsilon$ and 0.3 °C.

In our experimental demonstration, the measurement range was limited to ~8 m, which is expected to be elongated by using a temporal gating scheme [11].

References

[1] X. Bao, A. Brown, M. DeMerchant, and J. Smith, "Characterization of the Brillouin-loss spectrum of single-mode fibers by use of very short (< 10-ns) pulses," *Opt. Lett.*, vol. 24, no. 8, pp. 510–512, Apr. 1999.

[2] K. Y. Song, Z. He, and K. Hotate, "Distributed strain measurement with millimeter-order spatial resolution based on Brillouin optical correlation domain analysis," *Opt. Lett.*, vol. 31, no. 17, pp. 2526–2528, Sep. 2006.

[3] W. Zou, Z. He, and K. Hotate, "Complete discrimination of strain and temperature using Brillouin frequency shift and birefringence in a polarization-maintaining fiber," *Opt. Express*, vol. 17, no. 3, pp. 1248–1255, Feb. 2009.

[4] C. C. Lee, P. W. Chiang, and S. Chi, "Utilization of a dispersion-shifted fiber for simultaneous measurement of distributed strain and temperature through Brillouin frequency shift," *IEEE Photon. Technol. Lett.*, vol. 13, no. 10, pp. 1094–1096, Oct. 2001.

[5] L. Zou, X. Bao, and L. Chen, "Brillouin scattering spectrum in photonic crystal fiber with a partially germanium-doped core," *Opt. Lett.*, vol. 28, no. 21, pp. 2022–2024, Nov. 2003.

[6] W. Zou, Z. He, and K. Hotate, "Stimulated Brillouin scattering and its dependences on temperature and strain in a high-delta optical fiber with F-doped depressed inner cladding," *Opt. Lett.*, vol. 32, no. 6, pp. 600–602, Mar. 2007.

[7] W. Zou, Z. He, and K. Hotate, "Acoustic modal analysis and control in w-shaped triple-layer optical fibers with highly-germanium-doped core and F-doped inner cladding," *Opt. Express*, vol. 16, no. 14, pp. 10006–10017, Jul. 2008.

[8] K. Y. Song, W. Zou, Z. He, and K. Hotate, "All-optical dynamic grating generation based on Brillouin scattering in polarization-maintaining fiber," *Opt. Lett.*, vol. 33, no. 9, pp. 197–199, May 2008.

[9] W. Zou, Z. He, K. Y. Song, and K. Hotate, "Correlation-based distributed measurement of dynamic grating spectrum generated in stimulated Brillouin scattering in a polarization-maintaining optical fiber," *Opt. Lett.*, vol. 34, no. 7, pp. 1126–1128, Apr. 2009.

[10] K. Y. Song, W. Zou, Z. He, and K. Hotate, "Optical time-domain measurement of Brillouin dynamic grating spectrum in a polarization maintaining fiber," *Opt. Lett.*, vol. 34, no. 9, pp. 1381–1383, May 2009.

[11] M. Kannou, S. Adachi, and K. Hotate, "Temporal gating scheme for enlargement of measurement range of Brillouin optical correlation domain analysis for optical fiber distributed strain measurement," in *Proc. 16th Int. Conf. Optical Fiber Sensors (OFS16)*, Nara, Japan, Oct. 2003, pp. 454–457.